Isoform-Specific Lidocaine Block of Sodium Channels Explained by Differences in Gating

H. Bradley Nuss,† Nicholas G. Kambouris,* Eduardo Marbán,† Gordon F. Tomaselli,† and Jeffrey R. Balser*
*Division of Cardiac Anesthesia, Department of Anesthesiology and Critical Care Medicine, and †Section of Molecular and Cellular Cardiology, Department of Medicine, The Johns Hopkins University School of Medicine, Baltimore, Maryland USA

ABSTRACT When depolarized from typical resting membrane potentials ($V_{rest} \sim -90$ mV), cardiac sodium (Na) currents are more sensitive to local anesthetics than brain or skeletal muscle Na currents. When expressed in *Xenopus* oocytes, lidocaine block of hH1 (human cardiac) Na current greatly exceeded that of μ1 (rat skeletal muscle) at membrane potentials near V_{rest}, whereas hyperpolarization to -140 mV equalized block of the two isoforms. Because the isoform-specific tonic block roughly parallels the drug-free voltage dependence of channel availability, isoform differences in the voltage dependence of fast inactivation could underlie the differences in block. However, after a brief (50 ms) depolarizing pulse, recovery from lidocaine block is similar for the two isoforms despite marked kinetic differences in drug-free recovery, suggesting that differences in fast inactivation cannot entirely explain the isoform difference in lidocaine action. Given the strong coupling between fast inactivation and other gating processes linked to depolarization (activation, slow inactivation), we considered the possibility that isoform differences in lidocaine block are explained by differences in these other gating processes. In whole-cell recordings from HEK-293 cells, the voltage dependence of hH1 current activation was ~20 mV more negative than that of μ1. Because activation and closed-state inactivation are positively coupled, these differences in activation were sufficient to shift hH1 availability to more negative membrane potentials. A mutant channel with enhanced closed-state inactivation gating (μ1-R1441C) exhibited increased lidocaine sensitivity, emphasizing the importance of closed-state inactivation in lidocaine action. Moreover, when the depolarization was prolonged to 1 s, recovery from a "slow" inactivated state with intermediate kinetics (I_M) was fourfold longer in hH1 than in μ1, and recovery from lidocaine block in hH1 was similarly delayed relative to μ1. We propose that gating processes coupled to fast inactivation (activation and slow inactivation) are the key determinants of isoform-specific local anesthetic action.

INTRODUCTION

Local anesthetics (LAs) block sodium currents more potently during repetitive depolarizations (use-dependent block) than during infrequent stimuli from rest (tonic block) (Courtney, 1975). Modulated receptor models of LA action (Hondeghem and Katzung, 1977; Hille, 1977) have attributed the complex sodium channel blocking actions of lidocaine to distinct binding affinities for three conformational states (closed, open, inactivated). Na currents through cardiac Na channels are more sensitive to block by LAs than are brain or skeletal muscle Na currents (Nuss et al., 1995b; Wang et al., 1996b; Makielski et al., 1997), and this could be interpreted as isoform-specific (but gating-independent) structural differences in the lidocaine receptor. However, recent studies challenge this notion and suggest that isoform-specific gating differences underlie apparent variations in LA sensitivity (Wright et al., 1997).

To examine the mechanism of isoform-specific LA action, we measured tonic and use-dependent block by lidocaine in heterologously expressed sodium channels from rat skeletal muscle (μ1) and human heart (hH1). Our data support the notion that isoform-specific lidocaine block results from differences in gating rather than receptor differences; however, we find that the kinetics of recovery from lidocaine block are relatively insensitive to isoform differences in fast inactivation gating, indicating that other gating differences must critically influence isoform-specific local anesthetic action. In contrast to the original formulation of Hodgkin and Huxley (1952), activation, fast inactivation, and slow inactivation gating are now known to be linked functionally and structurally (Chahine et al., 1994; Yang and Horn, 1995; Yang et al., 1996; Chen et al., 1996; Aldrich et al., 1983; Armstrong and Bezanilla, 1977; Armstrong and Gilly, 1979). We find that differences in activation gating, by virtue of the tight coupling between activation and inactivation, are sufficient to explain isoform differences in voltage-dependent availability and, secondarily, lidocaine block. Moreover, differences in recovery from block are augmented when depolarization is prolonged, suggesting that slower inactivation processes may play a role in isoform-specific lidocaine action. Hence isoform-specific differences in lidocaine block are critically linked to differences in activation and slow inactivation, rather than differences in fast inactivation. Preliminary reports of these results have appeared in abstract form (Nuss et al., 1997, 1998).

Received for publication 21 June 1999 and in final form 5 October 1999.

Address reprint requests to Dr. Jeffrey R. Balser, Vanderbilt University School of Medicine, MRB II, Room 560, Nashville, TN 37232-6602. Tel.: 615-936-0277; Fax: 615-936-0456; E-mail: jeff.balser@mcmail.vanderbilt.edu.

0006-3495/00/01/200/11 $2.00

MATERIALS AND METHODS

Channel expression and electrophysiology

Voltage-dependent steady-state availability of whole-cell Na current (I_{Na}) was recorded from *Xenopus* oocytes, using a two-microelectrode voltage

clamp (Warner Instruments Corp., Hamden, CT) 24–48 h after injection of cRNAs coding for the α subunit of the rat skeletal muscle Na channel (μ1) or the human heart Na channel (hH1). Adult female *Xenopus laevis* (Nasco, Ft. Atkinson, WI) were anesthetized and oocytes were harvested as described previously (Nuss et al., 1995b). In all cases (μ1 and hH1), the rat brain β_1 subunit was coinjected in five- to sixfold molar excess. The bath solution was ND-96 (in mM: 96 NaCl, 2 KCl, 1 $MgCl_2$, 1.8 $CaCl_2$, 5 HEPES, pH 7.6 with NaOH). All recordings were obtained at room temperature (20–22°C). Currents were sampled at 5–10 kHz and low-pass-filtered at 1–2 kHz.

Recordings of I_{Na} for purposes of comparing μ1 and hH1 activation were performed under conditions of better voltage control, using small HEK-293 cells (average cell capacitance 21 ± 3 pF) stably transfected with hH1 or μ1. Na channel cDNA was subcloned into the *Hin*dIII-*Xba*I site of the vector GFPIRS for bicistronic expression of the channel protein and GFP reporter as previously described (Johns et al., 1997). Stable cells were maintained in Dulbecco's modified Eagle's medium (DMEM) supplemented with glucose (4.5 mg/L), fetal bovine serum (10%), penicillin/streptomycin (1%), and geneticin (500 mg/L). For electrophysiological recording, cells plated at low density were bathed in a modified Tyrode's solution composed of 135 mM NaCl, 4 mM KCl, 1 mM $MgCl_2$, 10 mM dextrose, 10 mM HEPES, 2 mM $CaCl_2$ (pH 7.3 with NaOH). Pipettes were filled with a solution containing cesium and fluoride to minimize background potassium and chloride currents (130 mM CsF, 10 mM CsCl, 10 mM HEPES, 10 mM EGTA, 1 mM $MgCl_2$, pH 7.3 with KOH). To avoid time-dependent shifts in the *I-V* curve due to intracellular dialysis (Wang et al., 1996a), all experiments were performed within 5 min of patch rupture. After fire polishing, pipettes had tip resistances of 4–6 MΩ when filled with the internal recording solution. Currents were filtered at 2 kHz, using a −3-dB, four-pole low-pass Bessel filter with <1% overshoot (Axopatch 200B; Axon Instruments). The sampling interval was 10 μs (100 data points/ms). Peak current amplitudes equaled −4.8 ± 0.6 nA, and series resistance compensation was 80–90% during all experiments. As such, the average uncompensated voltage error across the pipette was calculated to be 3.6 ± 0.4 mV.

All experiments were performed at room temperature. Voltage-clamp protocols are described in the Results section or in the appropriate figure legends. Pooled data are expressed as means ± SE. Between-group differences were compared using analysis of variance (Origin; MicroCal, Northampton, MA). Exponential (Figs. 2 and 5) and Boltzmann (Figs. 1 and 4) functions were fitted to the data with a nonlinear least-squares Marquardt-Levenberg algorithm (Origin).

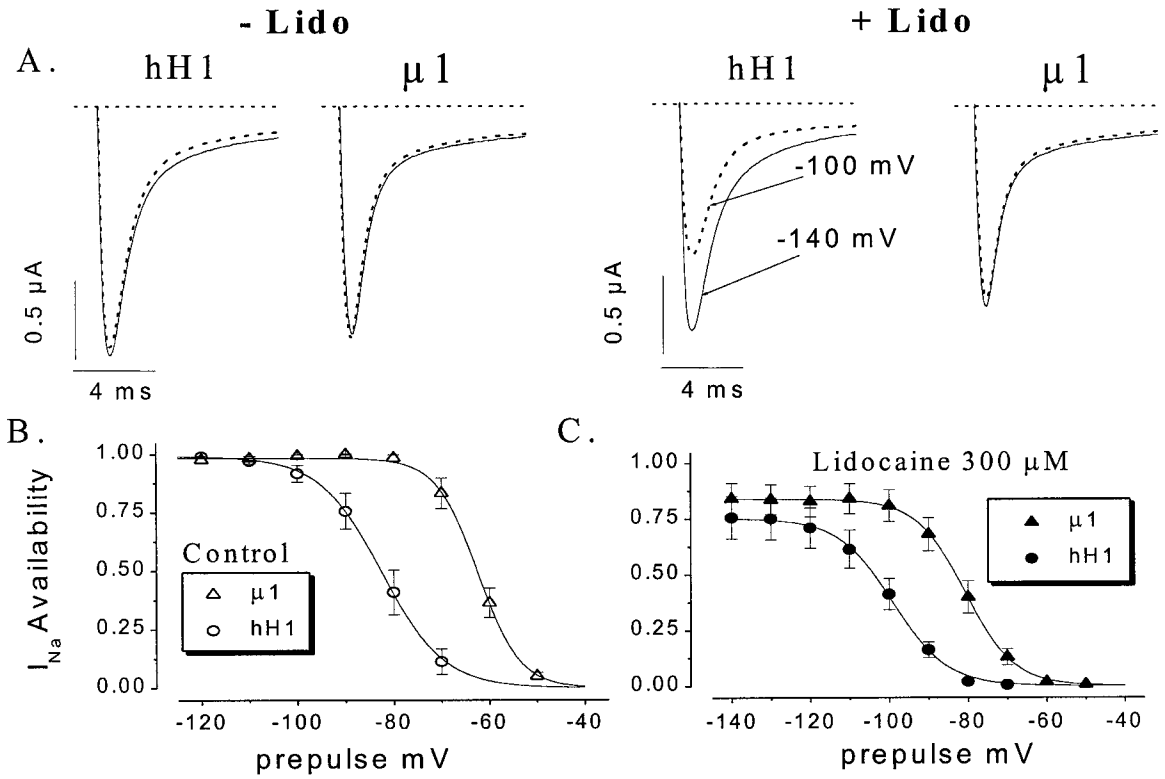

FIGURE 1 Isoform differences in tonic block. (*A*) Whole-oocyte currents (I_{Na}) recorded at −20 mV are shown from an oocyte expressing hH1 channels or μ1 channels after 5-s prepulse periods to either −140 mV (*solid lines*) or −100 mV (*dotted lines*). Capacity artifacts are blanked, and currents were not leak subtracted. Under drug-free conditions, the hH1 peak inward current magnitude was only slightly decreased by the more depolarized (−100 mV) prepulse. The same oocytes were then exposed to 300 μM lidocaine (*right*) and subjected to the same voltage-clamp protocols. The μ1 currents were reduced to the same extent after −140 mV and −100 mV prepulses; however, lidocaine block of the hH1 current was significantly augmented by the more depolarized (−100 mV) prepulse. (*B* and *C*) Drug-free (*B*) and drug-exposed (*C*) steady-state availability data were measured from peak I_{Na}. All data are from paired comparisons with drug-free controls in the same oocyte (μ1: 6 oocytes; hH1: 9 oocytes). Both drug-free and drug-exposed I_{Na} at each test potential were normalized to the drug-free I_{Na} recorded at −140 mV. I_{Na} was measured at −20 mV after a 5-s prepulse period at the test potential (−140 mV to −50 mV in 10-mV increments). Each prepulse period was preceded by a 15-s equilibration period at −100 mV. The solid lines are a least-squares fit of a Boltzmann function ($y = \{1 + \exp((V - V_{1/2})/\delta)\}^{-1}$) to the mean data. μ1 control: $V_{1/2} = -62.4$ mV, $\delta = 4.3$ μ1 lido: $V_{1/2} = -80.7$, $\delta = 6.2$; hH1 control: $V_{1/2} = -82.5$, $\delta = 6.5$ hH1 lido: $V_{1/2} = -99.0$, $\delta = 6.8$.

RESULTS

Isoform differences in voltage-dependent availability and tonic lidocaine block

We performed voltage-clamp experiments aimed at explicitly defining the isoform-specific differences in the voltage dependence of channel availability and tonic block. Fig. 1 *A* shows I_{Na} recorded at −20 mV after a prepulse to either −140 mV (*solid line*) or −100 mV (*dotted line*) in oocytes expressing either hH1 or μ1 channels. In drug-free conditions (*left*), the depolarized prepulse (−100 mV) caused little (hH1) or no (μ1) reduction in I_{Na} compared to the current measured from −140 mV. Fig. 1 *B* shows drug-free availability as a function of prepulse membrane potential for both isoforms. Fitting a Boltzmann function (*solid lines*) to the mean data indicated that half of the μ1 channels were unavailable at −62 mV, while $V_{1/2}$ for hH1 was −83 mV. Consistent with previous work (Nuss et al., 1995a; Wang et al., 1996a), we detect a 21-mV difference in the voltage dependence of I_{Na} availability for the two isoforms.

With exposure to lidocaine (Fig. 1 *A*, *right*), there was a small reduction in μ1 I_{Na} that was identical after prepulses to −140 mV and −100 mV. Furthermore, from a holding potential of −140 mV the lidocaine-induced reduction in hH1 I_{Na} was similar to that of μ1. In contrast, lidocaine markedly reduced hH1 I_{Na} after a prepulse to −100 mV. Examination of voltage-dependent I_{Na} availability during exposure to lidocaine (Fig. 1 *C*) confirmed that hH1 channels were far less available than μ1 channels after a prepulse to −100 mV (hH1: 41 ± 7% versus μ1: 80 ± 7%, $p = 0.002$), while at more hyperpolarized voltages (−140 mV) such differences were reduced (hH1: 75 ± 9% versus μ1: 84 ± 7%, $p = 0.52$). These findings are consistent with recent reports showing that isoform-specific local anesthetic tonic block generally parallels the isoform-specific difference in the voltage dependence of availability (Wright et al., 1997, 1999).

Although the parallel shift in drug-free availability and lidocaine action implicates depolarization-induced gating processes in isoform-specific block, the mechanistic underpinnings of this process remain unclear. This complexity was noted by Wright et al. (1999), who found that a simple two-affinity model (Bean et al., 1983) employing high and low-affinity binding to fast inactivated and rested states did not reliably predict the lidocaine-induced steady-state availability shifts in μ1/hH1 chimeras. In addition to fast inactivation, a number of coupled gating processes importantly contribute to the voltage dependence of channel availability, including activation and slow inactivation. Thus we considered the role of these individual gating processes relative to isoform-specific availability and lidocaine action.

Use-dependent block is relatively insensitive to isoform differences in fast inactivation

Voltage-clamp studies of I_{Na} in native cells (Bean et al., 1983) and with inactivation enzymatically (Yeh, 1978; Cahalan, 1978) or genetically removed (Bennett et al., 1995; Balser et al., 1996b) suggest that lidocaine binds with high affinity when channels inactivate. Use-dependent local anesthetic action has also been altered in Na channels with more subtle gating lesions that alter fast inactivation (An et al., 1996; Wang et al., 1997; Dumaine et al., 1996; Fan et al., 1996). Because hH1 and μ1 exhibit marked differences in recovery from fast inactivation (Wang et al., 1996a; Nuss et al., 1995a), we examined recovery after relatively brief prepulses to discern the effect of these gating differences on recovery from lidocaine block. A paired-pulse voltage clamp protocol (Fig. 2, *top*) was used to measure the rate of recovery of Na channel availability after a 50-ms depolarization to −20 mV. Fractional recovery (peak I_{Na} in the second pulse relative to the first) is plotted as a function of the recovery period at −100 mV (Fig 2 *A, left*) and −120 mV (Fig. 2 *B, left*). To facilitate visual comparison of the slow recovery components, the data are also shown for each recovery value after it has been normalized to the maximum fractional recovery within each experiment (Fig. 2, *right panels*). The solid lines (Fig. 2, *left panels*) show two-exponential fits to the unnormalized data (see Table 1 for fitted parameters). Under drug-free conditions (Fig. 2, *open symbols*), the rapid component of recovery, attributable to fast inactivation, was significantly faster for μ1 than for hH1, consistent with previous observations in both *Xenopus* oocytes (Nuss et al., 1995a) and mammalian cells (Wang et al., 1996a). At −100 mV, recovery from fast inactivation had a time constant of 1.07 ± 0.13 ms in μ1 versus 6.15 ± 0.91 msec in hH1 (Table 1, part B, $p < 0.05$). Following the predominant fast component, a small (low amplitude: Table 1, part A, $A_2 \approx 0.1$) slow component of recovery, attributable to one or more slow inactivated states (Nuss et al., 1995a, 1996), was kinetically indistinguishable in the two isoforms under these conditions (τ_2: Table 1, part C).

Lidocaine induced a substantial slow component of recovery in both isoforms (Fig. 2, *solid symbols*). The amplitude of the slow recovery component increased to a similar degree in the two isoforms (~0.65 in Table 1, part A, *solid symbols* at $t \geq 20$ ms in Fig. 2), and the time constants of slow recovery differed slightly (at −100 mV, τ_2 was somewhat greater in hH1; Table 1, part C; see comment in Discussion). Hence the overall time course of recovery in lidocaine (Fig. 2, *right panels*) was similar for the two isoforms, despite persistent differences in the kinetics of fast inactivation among the remaining fraction of unblocked channels. Notably, the amplitude of the fast recovery component in 200 μM lidocaine was still significant ($1 - A_2 \cong 0.35$), suggesting that the lidocaine receptor(s) were not saturated at this drug concentration.

Isoform differences in voltage-dependent availability reflect differences in activation

The shift in voltage-dependent availability between hH1 and μ1 is paralleled by a voltage-dependent shift in iso-

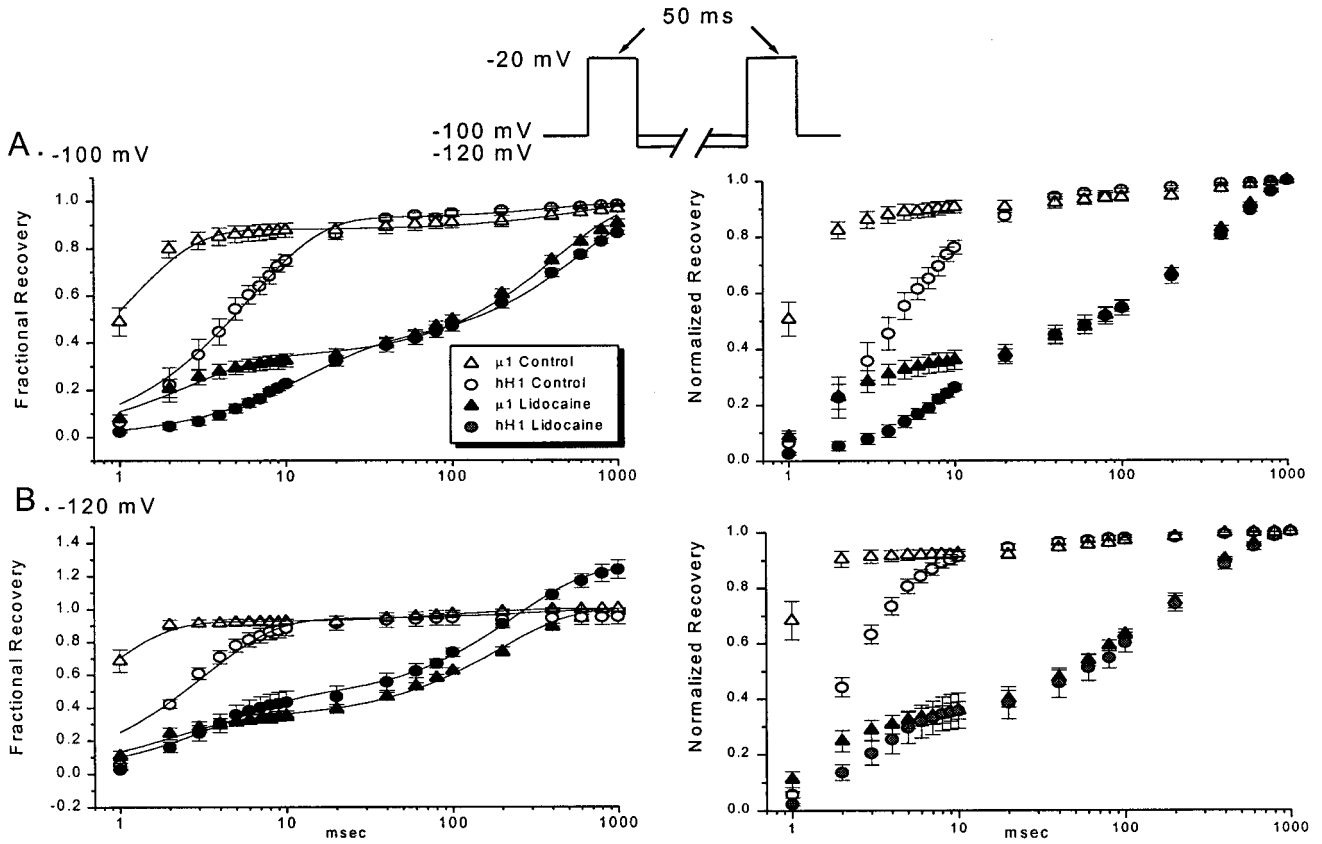

FIGURE 2 The lidocaine-induced delay in recovery of availability after a brief depolarization—fractional recovery of availability during repolarization at −100 mV (*A*) or −120 mV (*B*) after a brief (50 ms) depolarization (paired-pulse voltage-clamp protocol shown at top). Fractional recovery was measured as the ratio of peak I_{Na} in the second depolarizing pulse relative to the first and is plotted as a function of the repolarization interval (*left panels*). Because of isoform differences in steady-state availability, comparison of the slow recovery components was facilitated by normalizing each data point to the maximum (1 s) recovery value (*right panels*). The solid lines (*left panels*) show least-squares fits of a two-exponential function, $y = A_1(1 - \exp(-t/\tau_1)) + A_2(1 - \exp(-t/\tau_2))$ to the mean data, and Table 1 provides a summary of the parameters determined from fits to the individual experiments. Recovery for the two isoforms is shown in drug-free conditions (*open symbols*, −100 mV: μ1 ($n = 5$), hH1 ($n = 6$); −120 mV: μ1 ($n = 5$), hH1 ($n = 5$)) and with 200 μM lidocaine (*filled symbols*, −100 mV: μ1 ($n = 6$), hH1 ($n = 6$); −120 mV: μ1 ($n = 6$), hH1 ($n = 7$)). At both membrane potentials lidocaine induced a similar slow recovery component in μ1 and hH1.

form-specific block by lidocaine (Fig. 1) (Wright et al., 1997). Although differences in inactivation gating may partly underlie the isoform differences in voltage-dependent availability, because activation and inactivation gating are coupled, channel availability is heavily influenced by the voltage dependence of activation. Studies comparing hH1 and μ1 gating have shown a −15 mV-shift in the activation threshold for hH1 relative to μ1 (Nuss et al., 1995a; Wang et al., 1996a), a difference approaching the shift in steady-state availability for the two isoforms (−21 mV in Fig. 1 *B*). We therefore examined whether isoform-specific differences in the voltage dependence of activation could underlie the observed differences in voltage-dependent availability and lidocaine block.

If inactivation gating is mechanistically linked to activation, the two processes may be positively coupled such that closed-state inactivation becomes more likely as the Na channel partly activates with mild depolarization, as proposed by Kuo and Bean (1994):

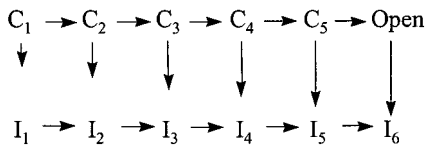

Scheme A

Scheme A predicts a delay of activation from "distant" nonconducting states (C_1, C_2) relative to the more rapid increase in macroscopic current when channels occupy more "proximal" closed states (C_3, C_4) (Cole and Moore, 1960). Because of positive coupling with inactivation, an isoform difference in voltage-dependent availability at "resting" membrane potentials ($V_{rest} \cong -90$ mV) would prevail if hH1 channels are further along their activation sequence at V_{rest} (i.e., C_3, C_4), while μ1 channels remain in more distal closed states (i.e., C_1, C_2). To test this prediction, we compared the rates of Na channel activation for hH1 and μ1 channels in HEK-293 cells.

TABLE 1 Parameters obtained from fitting the expression $y = A_1(1 - \exp(-t/\tau_1)) + A_2(1 - \exp(-t/\tau_2)$ to the experiments

	μ1	hH1	μ1 + lidocaine	hH1 + lidocaine
A. Slow recovery amplitude ($A_2/A_1 + A_2$)				
−100 mV	0.120 ± 0.03	0.087 ± 0.06	0.668 ± 0.02	0.630 ± 0.04
−120 mV	0.124 ± 0.02	0.064 ± 0.04	0.668 ± 0.02	0.652 ± 0.06
B. Time constant (τ_1, ms)				
−100 mV	1.07 ± 0.13	*6.15 ± 0.91	2.69 ± 0.38	*13.06 ± 2.84
−120 mV	0.71 ± 0.11	*3.21 ± 0.26	2.12 ± 0.29	*3.89 ± 0.51
C. Time constant (τ_2, ms)				
−100 mV	(621 ± 36)	(623 ± 173)	435 ± 108	*626 ± 56
−120 mV	(881 ± 108)	(1595 ± 700)	206 ± 22	314 ± 79

Parts A, B, and C list the parameters obtained from fitting the expression $y = A_1(1 - \exp(-t/\tau_1)) + A_2(1 - \exp(-t/\tau_2))$ to the individual experiments (unnormalized) represented in the left panels of Fig. 2. In part A, the amplitude of the slow recovery component is given as a fractional percentage of the total amplitude ($A_2/(A_1 + A_2)$). * indicates values derived from fitting the hH1 data that differ ($p < 0.05$) from the corresponding value in μ1. Because of the small amplitude of the slow recovery component (A_2) in drug-free conditions, the respective time constants (τ_2) are shown in parentheses (part C).

Fig. 3 shows representative current records from individual cells expressing hH1 (Fig. 3 *A*) or μ1 (Fig. 3 *B*) channels. For hH1, the rate of current activation is sensitive to changes in membrane potential positive to −140 mV (Fig. 3 *A, inset*; −130 mV current is shifted relative to −140 mV current) but saturates at membrane potentials positive to −100 mV (Fig. 3 *A, inset*; −100 mV and −90 mV currents superimpose). In the context of Scheme A, at membrane potentials positive to −100 mV, the hH1 channels occupy closed states so near to the open state that any additional movement along the activation sequence induces closed-state inactivation due to positive coupling. In contrast, the sensitivity of μ1 channel activation is shifted to more positive membrane potentials. The rate of current activation is insensitive until the membrane potential becomes positive to −130 mV (Fig. 3 *B, inset*; −140 mV and −130 mV currents superimpose) and does not saturate at −100 mV (Fig. 3 *B, inset*; even −90 mV and −80 mV currents are incrementally shifted). Summary data quantifying the dependence of activation rate on prepulse potential are provided in Fig. 3 *C*. The difference between the time to 50% activation (T50%) associated with the most negative (−140 mV) prepulse and that of the test prepulse is plotted for each isoform. In this way, ΔT50% indicates the degree to which the activation rate has increased with prepulse depolarization. Fig. 3 *C* indicates that the μ1 ΔT50% data were shifted positive to hH1 by ~20 mV. If activation and inactivation are positively coupled (e.g., Scheme A), these activation differences alone are sufficient to explain the isoform shift in voltage-dependent availability. Admittedly, a contribution from isoform differences in inactivation gating cannot be entirely excluded.

Lidocaine block of an S4 mutant that alters activation/inactivation coupling

Fig. 3 suggests that hH1 channels are further along the activation pathway than μ1 channels at the same holding potential. If this is correct, then according to the coupled gating scheme (Scheme A) proposed by Kuo and Bean (1994), more channels should undergo closed-state inactivation at a particular holding potential in hH1 compared to μ1. If we assume that this coupling paradigm between activation and closed-state inactivation is correct and lidocaine binds with high affinity to inactivated channels, then hH1 channels will exhibit greater lidocaine block at the same holding potential, as shown in Fig. 1. With a view to probing this scheme, the paradigm predicts lidocaine block should be sensitive to the extent of coupling between activation and closed-state inactivation. We therefore examined the lidocaine sensitivity of a μ1 channel with a mutation in the domain IV, S4 segment (R1441C) that alters activation/inactivation coupling (Chahine et al., 1994). Interestingly, this mutation disrupts coupling in a complex manner that reduces open-state inactivation but enhances closed-state inactivation (Ji et al., 1996). If lidocaine block is facilitated by closed-state inactivation, the mutant channel should exhibit enhanced drug sensitivity at holding potentials where closed-state inactivation is increased.

Fig. 4 shows a paired comparison of the lidocaine-induced shift in voltage-dependent availability for R1441C and wild-type μ1. Boltzmann fits to the mean availability data are shown by the solid lines, and parameters derived from fitting the individual experiments are provided in the figure legend. The R1441C channel exhibited reduced availability relative to wild type at −70 mV (R1441C: 0.84 ± 0.01, μ1: 0.99 ± 0.03, $p = 0.01$), a holding potential negative to the channel opening threshold where channels become unavailable by inactivating from closed states. We did not detect a shift in $V_{1/2}$ for the drug-free channels (μ1: −58.0 ± 0.5 mV; R1441C: −57.6 ± 1.5 mV), in contrast to the analogous mutation in hSkM1 (R1448C) when expressed in tsA201 cells (Ji et al., 1996). Although the lack of an effect on $V_{1/2}$ may reflect species differences (rat versus human) or the expression system (oocyte versus mammalian cell), the mutation-induced reduction in avail-

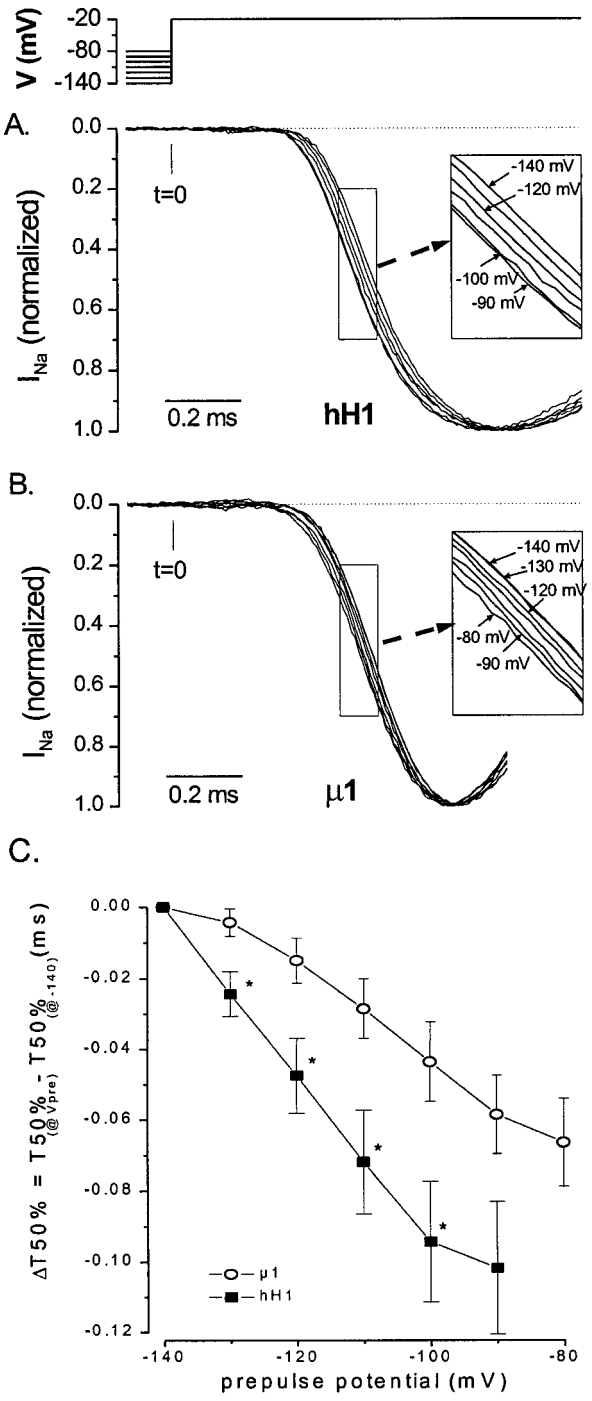

FIGURE 3 Activation of μ1 and hH1 Na channels. HEK-293 cells stably expressing hH1 (*A*) or μ1 (*B*) were held at −100 mV and subjected to 1-s prepulses to voltages from −140 mV to −80 mV in 10-mV increments (protocol, *top*). Currents were recorded upon depolarization to −20 mV. The insets amplify a 100-μs activation period for each isoform. (*C*) Plot of the time to 50% current activation (T50%) after holding at a range of depolarizing prepulse potentials relative to the same measurement at −140 mV. Summary data are shown for HEK-293 cells expressing hH1 (n = 8) and μ1 (n = 7). T50% is measured from time 0 (shown in *A* and *B*), at the onset of the voltage step to −20 mV, to the time at which the current attains 50% of its peak amplitude. * indicates membrane potentials where between-group differences were significant ($p < 0.05$).

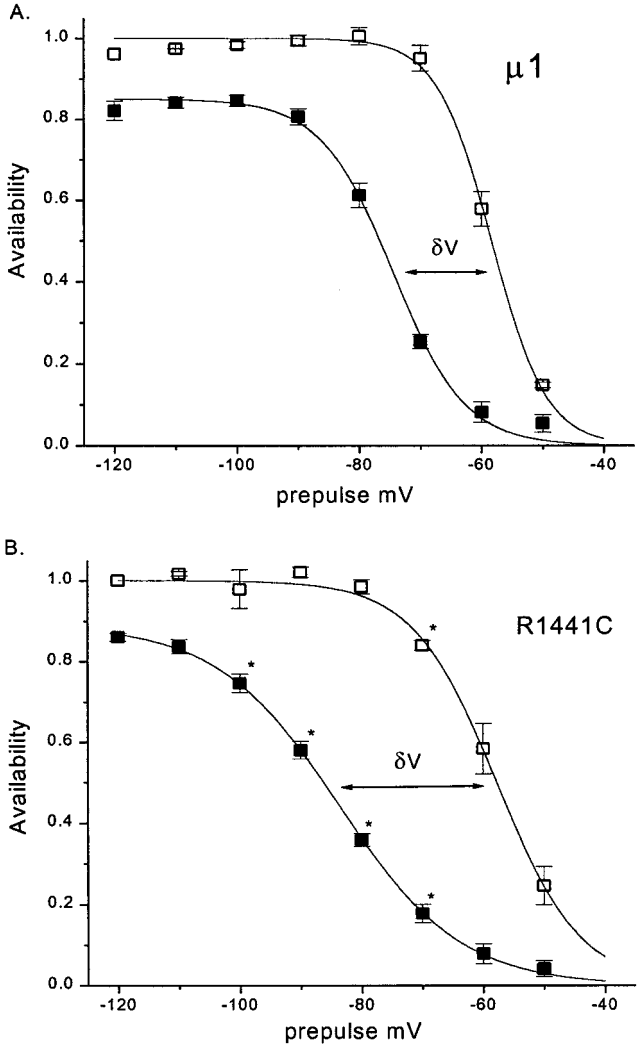

FIGURE 4 Voltage-dependent lidocaine block of μ1-R1441C. Voltage-dependent availability was measured using the voltage-clamp protocol from Fig. 1 in oocytes expressing wild type μ1 (n = 3) (*A*) and R1441C (n = 3) (*B*). Open symbols represent control data, and filled symbols show the results after paired exposure to lidocaine (300 μM). Solid lines are fits of the mean data to a Boltzmann function; parameters (mean ± SE) derived from fitting data from individual oocytes were as follows: wild type: $V_{1/2}$ = −58.0 ± 0.5 mV, δ = 4.2 ± 0.3; wild type + 300 μM lidocaine: $V_{1/2}$ = −73.5 ± 0.7 mV, δ = 5.3 ± 1.0; R1441C: $V_{1/2}$ = −57.6 ± 1.5 mV, δ = 6.7 ± 0.5; R1441C + 300 μM lidocaine: $V_{1/2}$ = −82.5 ± 1.1 mV, δ = 9.3 ± 1.2. Lidocaine induced a greater shift in $V_{1/2}$ for R1441C than wild type (see text).

ability at membrane potentials below the channel opening threshold supports an effect of R1441C on closed-state inactivation, consistent with the human isoform (Ji et al., 1996). In the absence of a shift in $V_{1/2}$, the reduced availability at membrane potentials negative to $V_{1/2}$ predicts that the fitted slope factor should increase, as was found (μ1: 4.2 ± 0.3; R1441C: 6.7 ± 0.5 mV, p = 0.012).

Lidocaine caused a reduction in voltage-dependent availability at membrane potentials below the opening threshold

(−70 to −100 mV) that was greater in R1441C than in wild-type μ1 (Fig. 4, *bottom*). Consistent with these results, lidocaine induced a greater shift in the fitted $V_{1/2}$ for R1441C (−24.1 ± 0.1 mV) than for wild-type μ1 (−15.5 ± 2.3 mV, $p = 0.016$). Hence, lidocaine block was increased by 1) isoform differences in coupling between activation and closed-state inactivation (Fig. 3) or 2) a mutation that alters coupling between activation and closed-state inactivation (Fig. 4). While these observations suggest that lidocaine block is sensitive to factors that modulate coupling between activation and closed-state inactivation, alternative mechanisms involving lidocaine binding directly to activated states are also possible (Vedantham and Cannon, 1999); they are considered below (Discussion).

Slow inactivation distinguishes isoform-specific use-dependent block

Figs. 3 and 4 suggest that differences in coupling between activation and closed-state inactivation underlie isoform differences in the voltage dependence of lidocaine block (Fig. 1). Nonetheless, Fig. 2 shows that the rate of recovery from lidocaine block after a brief (50 ms) depolarization is generally similar for hH1 and μ1, an apparent inconsistency given earlier evidence (Nuss et al., 1995b; Wang et al., 1996b) that use-dependent lidocaine block differs in the two isoforms. Notably, during sustained depolarizations (or rapid pulse trains that do not allow full recovery from inactivation), Na channels may enter stable (slow) inactivated states that are distinct from fast inactivation (Adelman and Palti, 1969; Chandler and Meves, 1970; Rudy, 1978). We have shown that mutation of a tryptophan in the outer pore of μ1 (W402A, W402C) attenuates entry into an inactivated state with intermediate recovery kinetics (denoted I_M) (Balser et al., 1996a; Kambouris et al., 1998a; Benitah et al., 1999). At the same time, mutation of this tryptophan speeds recovery from lidocaine block (Kambouris et al., 1998a). A recent report found that classic slow inactivation (induced by 60-s depolarizations, recovery time constants > 1 s) is less complete in hH1 than in the skeletal muscle isoform hSkM1 (see comments in Richmond et al., 1998). However, the kinetic features of I_M are distinct from classic slow inactivation: I_M is induced by shorter depolarizations (~1 s), and recovery from I_M has time constants of 100–300 ms in μ1 (Kambouris et al., 1998a; Benitah et al., 1999).

Fig. 5 compares recovery from inactivation for μ1 and hH1 after a 1-s depolarization (in contrast to Fig. 2, where only a 50-ms depolarization was used). The solid lines show exponential fits to the mean data (see legend); parameters obtained by fitting the individual experiments are provided in Table 2. In addition to the isoform differences in recovery from fast inactivation already noted with brief depolarizations (Fig. 2), a slow recovery component was amplified by the more lengthy depolarization that is consistent with I_M. In the absence of lidocaine (Fig. 5, *open symbols*), this slow component was more pronounced in hH1 than in μ1. While the amplitude (A_2) may have been slightly increased in hH1 compared to μ1 (0.19 ± 0.01 vs. 0.14 ± 0.02, $p = 0.06$), the time constant of slow recovery (τ_2) was more than fourfold longer in hH1 (719 ± 105 ms versus 145 ± 16 ms, $p < 0.001$, *left bars* in Fig. 5 *B*). Upon exposure to lidocaine, the amplitude of the slow component of recovery was increased in both isoforms, and in contrast to Fig. 2 the isoform difference in the rate of slow recovery persisted. The time constant of the drug-induced slow recovery component was significantly longer in hH1 than in μ1 (581 ±

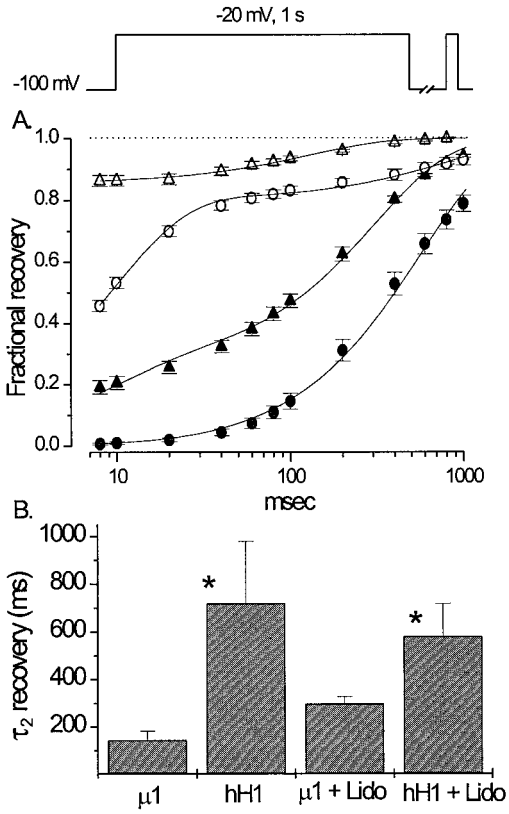

FIGURE 5 Time course of recovery of availability after a prolonged depolarization. The paired-pulse voltage clamp protocol is shown (*top*). Fractional recovery from inactivation was measured after a 1-s depolarization in oocytes expressing either μ1 (△) or hH1 (○) channels using control (○, △) or lidocaine-containing solutions (●, ▲). Although the lidocaine concentration was 700 μM for μ1 and 300 μM for hH1, recovery of μ1 was still considerably more rapid than recovery of hH1. The exponential function $y = A_1(1 - \exp(-t/\tau_1)) + A_2(1 - \exp(-t/\tau_2))$ was fitted to the mean recovery data (*solid lines*), and parameters obtained by fits to the individual experiments are shown in Table 2. Recovery was assessed using a minimum repriming interval of 8 ms at −100 mV, so a time constant for recovery from fast inactivation (τ_1) was not estimated precisely. The numbers of oocytes were as follows: μ1, $n = 5$; μ1 + lidocaine, $n = 6$; hH1, $n = 6$; hH1 + lidocaine, $n = 8$. Elements of the data were taken from previous work (Kambouris et al., 1998a; Nuss et al., 1995b). (*B*) The time constants for recovery from inactivation (from Table 2) are plotted for drug-free conditions (*left*) and in lidocaine (*right*). In either case, * indicates that the recovery time constant for hH1 was signficantly longer that that of μ1 ($p < 0.001$).

TABLE 2 Parameters obtained from fitting an exponential function to the individual experiments in Fig. 5.

	$(A_2/A_1 + A_2)$		τ_2 (ms)	
	μ1	hH1	μ1	hH1
Control	0.144 ± 0.02	0.194 ± 0.01	145 ± 16	*719 ± 105
Lidocaine	0.695 ± 0.04	~1.0	298 ± 29	*581 ± 47

* indicates values derived from fitting the hH1 data that differ ($p < 0.001$) from the corresponding value in μ1.

47 ms versus 298 ± 11 ms, $p < 0.001$, Fig. 5 *B, right bars*), despite exposure of the μ1 channel to more than twice the drug concentration. For the hH1 channel, the rapid recovery component was entirely eliminated (Fig. 5 *A*), while in μ1 a small-amplitude (0.26) rapid component of recovery remained. These findings suggest that differences in slow inactivation gating influence isoform-specific lidocaine block during periods of sustained depolarization.

DISCUSSION

Gating processes coupled to fast inactivation influence isoform-specific lidocaine block

Isoform differences in Na current sensitivity to lidocaine have been interpreted as intrinsic differences in the local anesthetic receptor (Nuss et al., 1995b; Wang et al., 1996b; Makielski et al., 1997). However, our results (Fig. 1) and those of others (Wright et al., 1997) indicate that such differences track voltage-dependent availability, implicating gating factors rather than receptor affinity in isoform-specific block. Based on this finding alone, it is impossible to conclude which of the gating processes that determine voltage-dependent availability actually underlies the isoform difference in lidocaine block. A recent analysis utilizing μ1/hH1 chimeras (Wright et al., 1999) suggested that gating mechanisms other than fast inactivation may contribute to isoform-specific local anesthetic action. Because voltage-dependent availability reflects an interaction among several "linked" gating processes (activation, fast inactivation, slow(er) inactivation), we considered the roles of each of these processes in isoform-specific block. Our results suggest that fast inactivation gating alone poorly explains isoform-specific lidocaine block: after a brief depolarization (50 ms), the two isoforms exhibit little difference in recovery from lidocaine block, despite marked kinetic differences in recovery from fast inactivation (Fig. 2).

Fig. 3 hints that isoform differences in voltage-dependent availability may be linked to differences in activation gating. The rate of hH1 current activation is shifted more by prepulse depolarization than is μ1 (Fig. 3 *C*), suggesting the hH1 channel resides in a more "activated" or "proximal" closed state (Scheme A: C_3 or C_4) during prepulse depolarizations near V_{rest}. If activation and inactivation are positively coupled, the depolarized hH1 channel is more likely to inactivate from a closed state. Could increased hH1 lidocaine sensitivity at modestly depolarized potentials therefore result from enhanced closed-state inactivation? A μ1 mutant with enhanced closed-state inactivation gating kinetics (R1441C; Fig. 4) produced a greater lidocaine-induced hyperpolarizing shift in voltage-dependent availability. Consistent with this finding, we have recently found that a disease-linked mutation of the analogous S4 residue in hH1 (R1623Q) similarly augments both closed-state inactivation and the lidocaine-induced shift in voltage-dependent availability (Kambouris et al., 1998b). Moreover, lidocaine block was stabilized by the homologous cysteine mutation in hSkM1 (Fan et al., 1996).

A model that considers slow inactivation in lidocaine block

Our findings (Figs. 2 and 5) indicate that prolonging the depolarization period from 50 ms to 1 s increases the isoform difference in recovery from lidocaine block. Importantly, after the longer depolarization the time constant of slow recovery in both the absence (Fig. 5 *B, left*) and presence (Fig. 5 *B, right*) of lidocaine was prolonged in the cardiac isoform. The recognition that lidocaine block may be mechanistically linked to a slow inactivation gating process (Kambouris et al., 1998a; Khodorov et al., 1976; Balser et al., 1996c; Zilberter et al., 1991) offers a means to explain this difference.

Fig. 6 proposes gated-state pathways for recovery of availability after either a short (*left*) or long (*right*) depolarization when lidocaine is bound to the channel. During a short depolarization, channels would primarily occupy the I_F state. Our findings are consistent with earlier reports showing that recovery from I_F is considerably delayed for hH1 relative to μ1 (Fig. 2 *A*, Table 1, part B) (Nuss et al., 1995a; Wang et al., 1996a). However, if the rate constant for lidocaine unbinding is slow relative to the rate of recovery from I_F, then the rate of drug unbinding will prevail over the isoform difference in gating to determine the overall rate of recovery of availability in lidocaine. Although the overall time courses of recovery from block in the two isoforms were similar (Fig. 2), the slow time constant in lidocaine was somewhat longer for hH1 at −100 mV (Table 1, part C). This difference could partly reflect an effect of fast inactivation gating differences (Table 1, part B) on the slow recovery time course. However, a low-amplitude slow inactivation component (consistent with I_M) was consistently present in drug-free conditions even after the short prepulse in both isoforms (Table 1, part A). The rather small amplitude of this component in drug-free conditions limited our ability to detect an isoform difference in τ_2 (reflecting I_M stability) after these short prepulses. Nonetheless, given that a marked isoform difference in I_M stability was established by using longer prepulses (Fig. 5), the small isoform difference in lidocaine recovery after short prepulses may well

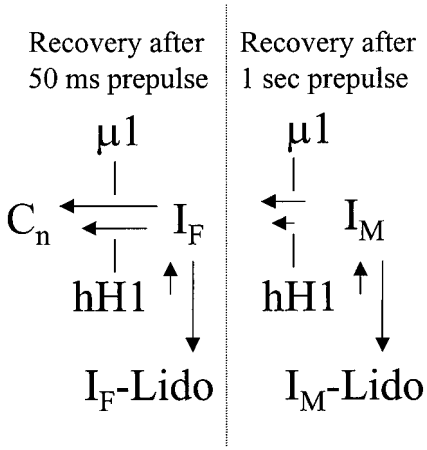

FIGURE 6 A model for isoform-specific use-dependent lidocaine block. The state model shows relative magnitudes of the recovery rate constants for the two isoforms. After a brief (50 ms) depolarization, channels primarily undergo fast inactivation, so the lidocaine-bound state is mainly I_F-Lido, and recovery occurs via I_F-Lido $\rightarrow I_F \rightarrow C_n$. In this case, the rate-limiting step is drug unbinding (I_F-Lido $\rightarrow I_F$), so differences in the rate of recovery from fast inactivation have little impact on the overall rate of recovery from block. In contrast, after a longer (1 s) prepulse, a substantial number of channels enter the I_M state, so recovery of availability now includes the pathway I_M-Lido $\rightarrow I_M \rightarrow I_F \rightarrow C_n$. Recovery from I_M ($I_M \rightarrow I_F$) is slow enough to influence the rate of recovery from block; hence the isoform difference in recovery from I_M (Fig. 5 *B*) renders use-dependent lidocaine block isoform-dependent.

reflect a limited degree of drug binding to the I_M state, even under these conditions.

After a longer depolarization (Fig. 5), a larger fraction of channels occupy I_M in drug-free conditions. While slightly more hH1 than μ1 channels may enter I_M (Fig. 5 *A*), the major difference between the isoforms lies in the time constant of recovery from I_M, which is more than fourfold slower for hH1 (Fig. 5 *B, left*, Table 2). With lidocaine exposure during a longer, 1-s prepulse, Fig. 6 predicts that the rate of recovery from block will be influenced by the rate of recovery from the drug-free I_M state because this rate is slow compared to drug unbinding or recovery from fast inactivation. Hence the isoform difference in the time constant for recovery from I_M with lidocaine present recapitulates those differences seen in drug-free conditions, as illustrated by Fig. 5 *B*.

In Fig. 6, we propose that the slow inactivated state is entered sequentially after fast inactivation, analogously to the model utilized in a recent study of slow inactivation in hH1 with varying external [Na^+] (Townsend and Horn, 1997). Admittedly, most evidence suggests that "classic" slow inactivation (Rudy, 1978; Featherstone et al., 1996), with time constants of recovery on the order of seconds (see figure 7A of Featherstone et al.), competes with fast inactivation. In this case a model with parallel (rather than sequential) entry into the fast and slow inactivated states would be preferable. However, the inactivated state considered here (I_M) has more "intermediate" kinetics (hundreds of milliseconds) compared to classic slow inactivation, and removal of fast inactivation (by an IFM $\rightarrow$ QQQ mutation in the III-IV linker) slows entry into I_M (Balser et al., 1996a), consistent with sequential coupling.

A recent study found that lidocaine did not slow the rate at which a cysteine placed in the III-IV linker fast inactivation "latch" recovered accessibility to covalent modification, suggesting that slow recovery from lidocaine block does not require fast inactivation gate "trapping" (Vedantham and Cannon, 1999). It was postulated that "activated" channels, rather than fast inactivated channels, may provide a high-affinity lidocaine receptor during brief (20 ms) depolarizations. Because the S4 mutation (R1441C) that augments closed-state inactivation also has subtle effects on activation gating, a model that includes activated-state lidocaine block would presumably be consistent with the data presented in Fig. 4. At present, a number of studies support roles for either activated channels (Wang et al., 1987; McDonald et al., 1989; Yeh and Tanguy, 1985; Vedantham and Cannon, 1999) or fast inactivated channels (Bennett et al., 1995; Cahalan, 1978; Yeh, 1978; Bean et al., 1983; Balser et al., 1996b) as high-affinity lidocaine receptors in various experimental conditions. In the model we propose (Fig. 6), high-affinity lidocaine binding to activated or open channels (rather than I_F) could suffice to explain the similar use-dependent block noted in the two isoforms after brief (50 ms) depolarizations (Fig. 2). Nonetheless, it is difficult to reconcile the isoform differences in lidocaine block that we observe during long (1 s) depolarizations (Fig. 5) with high-affinity binding to "activated" channels, because the depolarized Na channel inactivates within only a few milliseconds. Hence our data are consistent with previous studies (Khodorov et al., 1976; Zilberter et al., 1991; Balser et al., 1996c; Kambouris et al., 1998a) supporting the general hypothesis that slow inactivation, in addition to fast inactivated or activated states, forms a high-affinity lidocaine receptor. In summary, our findings suggest that isoform-specific differences in lidocaine block are well explained by isoform-specific differences in the gating processes coupled to fast inactivation (activation and slow inactivation), rather than intrinsic differences in fast inactivation or "structural" differences in the drug receptors per se.

This work was supported by the National Institutes of Health (R01 GM56307 to JRB, R01 HL52768 to EM, R01 HL50411 to GFT) and a grant-in-aid from the American Heart Association (Maryland Affiliate, JRB). Salary support was provided by the Clinician Scientist Award of the American Heart Association (JRB) and a NASPE fellowship grant (HBN).

REFERENCES

Adelman, W. J., and Y. Palti. 1969. The effects of external potassium and long duration voltage conditioning on the amplitude of sodium currents in the giant axon of the squid, *Loligo pealei. J. Gen. Physiol.* 54: 589–606.

Aldrich, R. W., D. P. Corey, and C. F. Stevens. 1983. A reinterpretation of mammalian sodium channel gating based on single channel recording. *Nature.* 306:436–441.

An, R. H., R. Bangalore, S. Z. Rosero, and R. S. Kass. 1996. Lidocaine block of LQT-3 mutant human Na channels. *Circ. Res.* 79:103–108.

Armstrong, C. M., and F. Bezanilla. 1977. Inactivation of the sodium channel. II. Gating current experiments. *J. Gen. Physiol.* 70:567–590.

Armstrong, C. M., and W. F. Gilly. 1979. Fast and slow steps in the activation of sodium channels. *J. Gen. Physiol.* 74:691–711.

Balser, J. R., H. B. Nuss, N. Chiamvimonvat, M. T. Perez-Garcia, E. Marban, and G. F. Tomaselli. 1996a. External pore residue mediates slow inactivation in μ1 rat skeletal muscle sodium channels. *J. Physiol. (Lond.).* 494:431–442.

Balser, J. R., H. B. Nuss, D. W. Orias, D. C. Johns, E. Marban, G. F. Tomaselli, and J. H. Lawrence. 1996b. Local anesthetics as effectors of allosteric gating: lidocaine effects on inactivation-deficient rat skeletal muscle Na channels. *J. Clin. Invest.* 98:2874–2886.

Balser, J. R., H. B. Nuss, D. N. Romashko, E. Marban, and G. F. Tomaselli. 1996c. Functional consequences of lidocaine binding to slow-inactivated sodium channels. *J. Gen. Physiol.* 107:643–658.

Bean, B. P., C. J. Cohen, and R. W. Tsien. 1983. Lidocaine block of cardiac sodium channels. *J. Gen. Physiol.* 81:613–642.

Benitah, J. P., Z. Chen, J. Balser, G. F. Tomaselli, and E. Marban. 1999. Molecular dynamics of the sodium channel pore vary with gating: interactions between P-segment motions and inactivation. *J. Neurosci.* 19:1577–1585.

Bennett, P. B., C. Valenzuela, C. Li-Qiong, and R. G. Kallen. 1995. On the molecular nature of the lidocaine receptor of cardiac Na^+ channels. *Circ. Res.* 77:584–592.

Cahalan, M. D. 1978. Local anesthetic block of sodium channels in normal and pronase-treated squid axons. *Biophys. J.* 23:285–311.

Chahine, M., A. L. George, M. Zhou, S. Ji, W. Sun, R. Barchi, and R. Horn. 1994. Sodium channel mutations in paramyotonia congenita uncouple inactivation from activation. *Neuron.* 12:281–294.

Chandler, W. K., and H. Meves. 1970. Slow changes in membrane permeability and long lasting action potentials in axons perfused with fluoride solutions. *J. Physiol. (Lond.).* 211:707–728.

Chen, L. Q., V. Santarelli, R. Horn, and R. G. Kallen. 1996. A unique role for the S4 segment of domain 4 in the inactivation of Na channels. *J. Gen. Physiol.* 108:549–556.

Cole, K. S., and J. W. Moore. 1960. Potassium ion current in the squid giant axon: dynamic characteristic. *Biophys. J.* 1:1–14.

Courtney, K. R. 1975. Mechanism of frequency-dependent inhibition of sodium currents in the frog myelinated nerve by the lidocaine derivative gea 968. *J. Pharmacol. Exp. Ther.* 195:225–236.

Dumaine, R., Q. Wang, M. T. Keating, H. A. Hartmann, P. J. Schwartz, A. M. Brown, and G. E. Kirsch. 1996. Multiple mechanisms of Na^+ channel-linked long-QT syndrome. *Circ. Res.* 78:916–924.

Fan, Z., A. L. George, J. W. Kyle, and J. C. Makielski. 1996. Two human paramyotonia congenita mutations have opposite effects on lidocaine block of Na^+ channels expressed in a mammalian cell line. *J. Physiol. (Lond.).* 496:275–286.

Featherstone, D. E., J. E. Richmond, and P. C. Ruben. 1996. Interaction between fast and slow inactivation in Skm1 sodium channels. *Biophys. J.* 71:3098–3109.

Hille, B. 1977. Local anesthetics: hydrophilic and hydrophobic pathways for the drug-receptor reaction. *J. Gen. Physiol.* 69:497–515.

Hodgkin, A. L., and A. F. Huxley. 1952. A quantitative description of membrane current and its application to conduction and excitation in nerve. *J. Physiol.* 117:500–544.

Hondeghem, L. M., and B. G. Katzung. 1977. Time- and voltage-dependent interactions of the antiarrhythmic drugs with cardiac sodium channels. *Biochim. Biophys. Acta.* 472:373–398.

Ji, S., A. L. George, R. Horn, and R. L. Barchi. 1996. Paramyotonia congenita mutations reveal different roles for segments S3 and S4 of domain D4 in hSkM1 sodium channel gating. *J. Gen. Physiol.* 107: 183–194.

Johns, D. C., H. B. Nuss, and E. Marban. 1997. Suppression of neuronal and cardiac transient outward currents by viral gene transfer of dominant negative KV4.2 constructs. *J. Biol. Chem.* 272:31598–31603.

Kambouris, N., L. Hastings, S. Stepanovic, E. Marban, G. F. Tomaselli, and J. R. Balser. 1998a. Mechanistic link between local anesthetic action and inactivation gating probed by outer pore mutations in the rat μ1 sodium channel. *J. Physiol. (Lond.).* 512:693–705.

Kambouris, N. G., H. B. Nuss, D. C. Johns, G. F. Tomaselli, and J. R. Balser. 1998b. Single-channel analysis of lidocaine action in hH1 Na channels containing the R1623Q mutation. *Circulation.* 98:I-467.

Khodorov, B., L. Shishkova, E. Peganov, and S. Revenko. 1976. Inhibition of sodium currents in frog Ranvier node treated with local anesthetics: role of slow sodium inactivation. *Biochim. Biophys. Acta.* 433:409–435.

Kuo, C. C., and B. P. Bean. 1994. Na^+ channels must deactivate to recover from inactivation. *Neuron.* 12:819–829.

Makielski, J. C., J. Limberis, Z. Fan, and J. W. Kyle. 1997. Isoform and β1 subunit effects on lidocaine affinity for human heart and skeletal muscle Na channels expressed in oocytes. *PACE Pacing Clin. Electrophysiol.* 20:1217.

McDonald, T. V., K. R. Courtney, and W. T. Clusin. 1989. Use-dependent block of single sodium channels by lidocaine in guinea pig ventricular myocytes. *Biophys. J.* 55:1261–1266.

Nuss, H. B., J. R. Balser, D. W. Orias, J. H. Lawrence, G. F. Tomaselli, and E. Marban. 1996. Coupling between fast and slow inactivation revealed by analysis of a point mutation (F1304Q) in μ1 rat skeletal muscle sodium channels. *J. Physiol. (Lond.).* 494:411–429.

Nuss, H. B., N. Chiamvimonvat, M. T. Perez-Garcia, G. F. Tomaselli, and E. Marban. 1995a. Functional association of the β_1 subunit with human cardiac (hH1) and rat skeletal muscle (μ1) sodium channel α subunits expressed in *Xenopus* oocytes. *J. Gen. Physiol.* 106:1171–1191.

Nuss, H. B., N. G. Kambouris, D. C. Johns, E. Marban, G. F. Tomaselli, and J. R. Balser. 1998. Isoform-specific lidocaine block of sodium channels rationalized by differences in activation gating. *Circulation.* 98:I-54.

Nuss, B., N. G. Kambouris, G. F. Tomaselli, E. Marban, and J. R. Balser. 1997. Isoform-specific differences in gating underlie the enhanced susceptibility of cardiac sodium channels to lidocaine. *Circulation.* 96:I-120.

Nuss, H. B., G. F. Tomaselli, and E. Marban. 1995b. Cardiac sodium channels (hH1) are intrinsically more sensitive to tonic block by lidocaine than are skeletal muscle (μ1) channels. *J. Gen. Physiol.* 106:1193–1210.

Richmond, J. E., D. E. Featherstone, H. A. Hartmann, and P. C. Ruben. 1998. Slow inactivation in human cardiac sodium channels. *Biophys. J.* 74:2945–2952.

Rudy, B. 1978. Slow inactivation of the sodium conductance in squid giant axons. Pronase resistance. *J. Physiol. (Lond.).* 238:1–21.

Townsend, C., and R. Horn. 1997. Effect of alkali metal cations on slow inactivation of cardiac Na channels. *J. Gen. Physiol.* 110:23–33.

Vedantham, V., and S. C. Cannon. 1999. The position of the fast-inactivation gate during lidocaine block of voltage-gated Na+ channels. *J. Gen. Physiol.* 113:7–16.

Wang, D. W., A. L. George, and P. B. Bennett. 1996a. Comparison of heterologously expressed human cardiac and skeletal muscle sodium channels. *Biophys. J.* 70:238–245.

Wang, D. W., L. Nie, A. L. George, and P. B. Bennett. 1996b. Distinct local anesthetic affinities in Na^+ channel subtypes. *Biophys. J.* 70:1700–1708.

Wang, D. W., K. Yazawa, N. Makita, A. L. George, and P. B. Bennett. 1997. Pharmacological targeting of long QT mutant sodium channels. *J. Clin. Invest.* 99:1714–1720.

Wang, G. K., M. S. Brodwick, D. C. Eaton, and G. R. Strichartz. 1987. Inhibition of sodium currents by local anesthetics in chloramine-T-treated squid axons: the role of channel activation. *J. Gen. Physiol.* 89:645–667.

Wright, S. N., S. Wang, R. G. Kallen, and G. K. Wang. 1997. Differences in steady-state inactivation between Na channel isoforms affect local anesthetic binding affinity. *Biophys. J.* 73:779–788.

Wright, S. N., S. Y. Wang, Y. F. Xiao, and G. K. Wang. 1999. State-dependent cocaine block of sodium channel isoforms, chimeras, and channels coexpressed with the beta1 subunit. *Biophys. J.* 76:233–245.

Yang, N., A. L. George, and R. Horn. 1996. Molecular basis of charge movement in voltage-gated sodium channels. *Neuron.* 16:113–122.

Yang, N., and R. Horn. 1995. Evidence for voltage-dependent S4 movement in sodium channels. *Neuron.* 15:213–218.

Yeh, J. Z. 1978. Sodium inactivation mechanism modulates qx-314 block of sodium channels. *Biophys. J.* 24:569–574.

Yeh, J. Z., and J. Tanguy. 1985. Na channel activation gate modulates slow recovery from use-dependent block by local anesthetics in squid giant axons. *Biophys. J.* 47:685–94.

Zilberter, Y., L. Motin, S. Sokolova, A. Papin, and B. Khodorov. 1991. Ca-sensitive slow inactivation and lidocaine-induced block of sodium channels in rat cardiac cells. *J. Mol. Cell. Cardiol.* 23:61–72.